On the Possibility of Non-Neutral Antiproton Plasmas and Antiproton-Positron Plasmas

H. Higaki

Plasma Research Center, University of Tsukuba
1-1-1, Tennoudai, Tsukuba, Ibaraki, Japan 305-8577

Abstract. Progresses in accumulating a large number of low energy antiprotons with Antiproton Decelerator (AD), Radio Frequency Quadrupole Decelerator (RFQD), and a multiring trap in Atomic Spectroscopy And Collisions Using Slow Antiprotons (ASACUSA) enables the confinement of more than 10^6 antiprotons. Confinement of a larger number of antiprotons in the trap will result in a non-neutral antiproton plasma. This is also favorable for the effective production of low energy antiproton beams. Possibility of an antiproton-positron plasma is also considered in a magnetic mirror field.

Keywords: antiproton plasma, antiproton-positron plasma, magnetic mirror field
PACS : 52.27.Jt, 52.35.Fp, 52.55.Jd

INTRODUCTION

A large number of low energy antiprotons ($<10^5$) have been confined in particle traps at Antiproton Decelerator (AD) in CERN [1,2]. However, plasma oscillations of a non-neutral antiproton plasma have not been observed. It is thought that the size of the antiproton cloud was smaller than its Debye length. Progresses in accumulating a larger number of low energy antiprotons with AD, Radio Frequency Quadrupole Decelerator (RFQD), and a multiring trap in Atomic Spectroscopy And Collisions Using Slow Antiprotons (ASACUSA) enabled the confinement of a larger number of antiprotons ($>10^6$) [3]. Further improvement in stacking antiproton pulses will lead to the observation of the plasma oscillations of a non-neutral antiproton plasma. The large amount of antiprotons is also favorable for the effective production of low energy antiproton beams to be used in atomic collision experiments.

The possibility of producing antiproton-positron plasmas is also considered with a magnetic mirror configuration. Although antihydrogen atoms were created by mixing a positron plasma and antiproton cloud [2,4], it was a beam-plasma system. The basic procedure here is to accumulate both antiprotons and positrons in a nested Penning trap in a magnetic mirror field. It is assumed that more positrons are trapped than antiprotons. Adiabatic expansion of particles along the magnetic field by reducing the trapping potential results in an anisotropic energy distribution. Then, the positron plasma can be trapped with the magnetic mirror field and antiprotons can be trapped simultaneously with the magnetic field and the space potential of the positron plasma. A small power positron cyclotron resonance heating may enhance the confinement time of the antiproton-positron plasma.

CP793 *Physics with Ultra Slow Antiproton Beams*
edited by Yasunori Yamazaki and Michiharu Wada

ANTIPROTON PLASMAS

When a large number of charged particles are confined in a Penning trap, they behave as a non-neutral plasma. For examples, 4.3×10^4 electrons confined in a Penning trap in a cryogenic environment were characterized with its electrostatic electron plasma oscillations [5]. Unfortunately, such a small number of electrons are not enough for the effective cooling of high energy antiprotons provided through RFQD. A larger number of electrons ($>10^8$) with aspect ratio much larger than unity behaves as a prolate spheroidal plasma even if its temperature is larger than 1eV [6]. This spheroidal non-neutral electron plasma has been used to cool high energy protons [6] and antiprotons [3]. Since the frequencies of the electrostatic oscillations depend on the electron plasma temperature, non-destructive measurement of the frequencies works as a real time monitor of the electron cooling process.

There are also some examples of non-neutral ion plasmas. When a laser cooling technique is available, as in Be^+ ions [7], strongly coupled plasmas can be realized with the ion numbers less than 10^5. Otherwise, a larger number of ions are required in general to form ion plasmas of Li [8] and Mg [9], since the plasma temperature is not low enough.

As far as antiparticles are concerned, positron plasmas have been already realized with more than 10^7 positrons [10]. They were used for antihydrogen synthesis [2], low energy positron collision experiments [11], and so on. Positron plasmas are to be used for the cooling of highly charged ions [12]. However, there has been no report on the observation of plasma oscillations for antiproton plasmas. This might be because the temperature of antiprotons were not low enough that the estimated Debye length was larger than the cloud size, or the sensitivity of the detectors were not enough to detect the electrostatic oscillations of antiprotons.

Some parameters for above examples are listed in TABLE 1. Here, N, n, T, r, z, and λ_D, denote the particle number, density, temperature, radius, half axial length, and estimated Debye length, respectively.

TABLE 1. Various non-neutral plasmas and clouds.

Species	N	n [cm^{-3}]	T	r [mm]	z [mm]	λ_D [mm]
Electron [5]	4.3×10^4	4.5×10^7	~ 4 K	3.83	0.015	0.020
Electron [6]	1×10^8	3.5×10^7	< 1eV	4.6	30	1.3
Positron [10]	2×10^7	1×10^6	0.025eV	15	20	1
Be^+ [7]	6×10^4	2.7×10^9	20mK	0.12	0.38	0.0002
Li+ [8]	6.7×10^9	7.3×10^6	1.2eV	16	580	3
Mg+ [9]	10^9	3×10^7	0.05eV	10	50	0.3
Proton [13]	1×10^6	1.2×10^7	~ 5eV	1	20	5
Antiproton [3]	1×10^7	1.4×10^8	1eV ?	1	16	0.6 ?

As seen from above examples, one possibility to obtain antiproton plasmas is accumulating a large amount of low energy antiprotons in the trap. For the purpose of estimating the behavior of an antiproton cloud in the multiring trap, properties of ~ 10^6 protons were investigated in advance [13]. The trap is composed of 12 ring electrodes aligned along the uniform magnetic field [3,6]. A unique feature of the trap is the ability to confine a large number of electrons (> 10^8) in a large volume with a harmonic potential, so that a large number of high energy antiprotons (> 10^6) can be

cooled effectively. Since the production of low energy (< 1keV) antiproton beams in field free region is one of the main purposes of the multiring trap, the accumulated low energy antiprotons have to be extracted from the strong magnetic field through the transport beam line [14]. The crucial condition for the effective transport of low energy antiprotons is that the antiproton cloud (or plasma) should have small radial extent inside the trap. Thus, the radius of the antiproton cloud has to be controlled by the sideband cooling [5] or rotating electric field [9], depending on if it is a cloud or plasma. In case of 10^6 protons in the multiring trap, the temperature was unfortunately too high to be a plasma. Therefore, the sideband cooling was effective for the radial compression of proton clouds [13]. Only the center of mass motion was observed before and after the radial compression of the proton cloud, as shown in FIG.1.

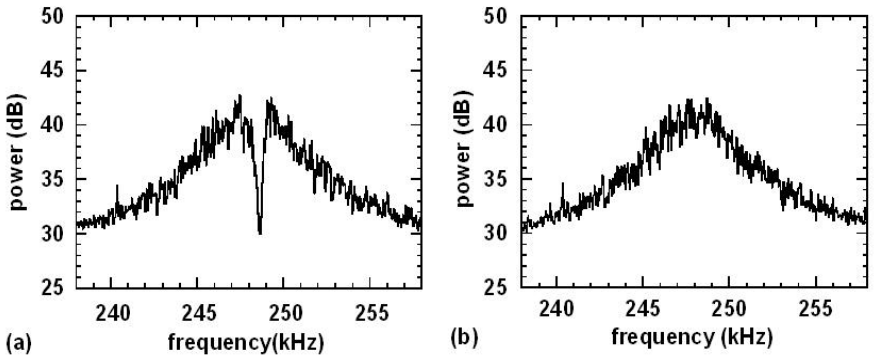

FIGURE 1. Tank circuit signals (a) with and (b) without 10^6 protons in the multiring trap before radial compression. After radial compression, the dip appeared in (a) shifts lower by 4 kHz.

What happened with antiprotons provided through RFQD was that 10^6 low energy antiprotons were confined routinely in the multiring trap. In this case, electrons can cool antiprotons less than 1 eV before electrons are discarded for the radial compression of antiprotons. Furthermore, some AD pulses are stacked to obtain a larger amount of antiprotons. Any improvements in the cooling efficiency in AD, RFQD, or multiring trap, and further progresses in stacking antiproton pulses from RFQD into the multiring trap will increase the number and volume of low energy antiprotons in the trap. As far as the radial compression takes much longer time compared with the AD cycle, stacking as many antiproton pulses as possible will reduce the waste of AD pulses. Currently, 10^7 slow antiprotons in the trap are foreseen. Depending on its temperature, the antiproton cloud can behave as a non-neutral plasma. For example, the temperature of 1eV after radial compression with the density of 1.4×10^8 cm^{-3} ($r_p \sim 1$mm, $z_p \sim 16$mm), results in the Debye length of about 0.6mm. This antiproton cloud should behave as a non-neutral plasma at least in the axial direction. Small amount of remnant electrons may help cooling antiprotons. Then, the electrostatic oscillation of the antiproton plasma should be observed near 400kHz with the normal experimental parameters of the multiring trap. This frequency may be shifted due to the remaining electrons. Detecting continuously the

second harmonic axial oscillation of antiproton plasma will be a powerful tool for the nondestructive measurement inside the multiring trap.

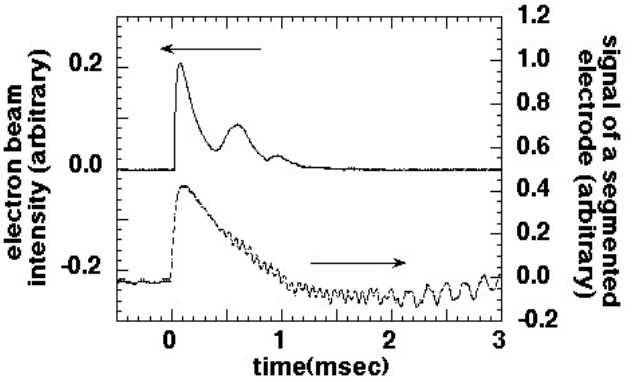

FIGURE 2. The electron beam intensity (solid line) fluctuates with diocotron oscillations (dashed line) when electrons are extracted with the time scale of a few msec.

Once antiproton plasmas are obtained, another problem may arise during their extraction. In the course of test experiments in the multiring trap with electron plasmas, depending on the duration of extraction, diocotron oscillations were observed and the extracted beam intensity fluctuated a lot. Shown in FIG.2 are the extracted electron beam intensity (solid line) and the signal obtained by an azimuthally segmented electrode (dashed line). It is seen that the later includes the fluctuations around10 kHz corresponding to diocotron oscillations. This implies that proper manipulations of antiproton plasmas will be also necessary for the effective production of low energy antiproton beams to be used in atomic collision experiments.

ANTIPROTON-POSITRON PLASMAS

As mentioned in the introduction, the simultaneous confinement of both antiprotons and positrons is considered with a magnetic mirror configuration. Since the plasma confinement in a magnetic mirror has been investigated more than decades for thermonuclear fusion, characteristics of the magnetic mirror confinement is presented before the confinement of a dilute antiproton-positron plasma is considered.

Brief Review of Magnetic Mirror Confinement

Principles of a single particle confinement in a magnetic mirror with the mirror ratio $R = B_1/B_0$ can be found in any textbooks on plasma physics [15]. Here, B_0 and B_1 denote the field strength at the center of the magnetic mirror (weakest) and at the mirror throats (strongest), respectively. The magnetic moment μ of a charged particle (charge:e, mass:m) in a magnetic field B is given by

$$\mu = IS = \frac{e\omega_c}{2\pi}\pi\rho^2 = \frac{mv_\perp^2}{2B} \tag{1}$$

with the cyclotron frequency ω_c, Larmor radius ρ, and the perpendicular velocity of the particle $v_\perp$. This magnetic moment is the adiabatic invariant under the condition that the magnetic field changes slowly, which, in this case, is expressed by

$$\omega_c << \frac{L}{v_{//}}. \tag{2}$$

Here, L denotes the scale length of the magnetic field gradient. The conservation of energy and magnetic moment in the magnetic mirror field gives the following equations.

$$\begin{aligned} \varepsilon &= m\frac{v_{//0}^2 + v_{\perp 0}^2}{2} = m\frac{v_0^2}{2} = m\frac{v_{//1}^2 + v_{\perp 1}^2}{2} \\ \mu &= \frac{mv_{\perp 0}^2}{2B_0} = \frac{mv_{\perp 1}^2}{2B_1} \end{aligned} \tag{3}$$

The axial confinement is provided if $v_{//1}^2 = 0$. Thus, the loss cone angle θ_0 is determined with the mirror ratio by the following equation.

$$\frac{1}{R} = \frac{B_0}{B_1} = \frac{v_{\perp 0}^2}{v_{\perp 1}^2} = \frac{v_{\perp 0}^2}{v_0^2} \equiv sin^2\theta_0 \tag{4}$$

It means that a particle is confined if the pitch angle θ at the center is larger than θ_0 and is lost if $\theta < \theta_0$. The gray region in FIG.3 is called loss cone. As an example, R=5 gives $\theta_0 \approx 27^o$.

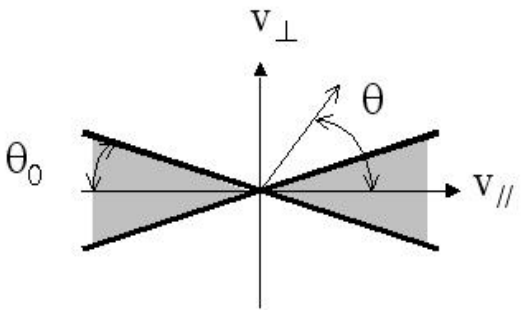

FIGURE 3. A single particle in a magnetic mirror. A particle with a pitch angle $\theta < \theta_0$ is not confined with the mirror ratio $R = 1/\sin^2\theta_0$.

When a plasma composed of protons and electrons is confined in a simple magnetic mirror, the loss cone is modified due to its self field potential $\phi(z)$. The conservation of energy and magnetic moment are given by the following equations.

$$\begin{aligned} \varepsilon &= m\frac{v_{//}^2 + v_\perp^2}{2} + e\,\phi(z) = const. \\ \mu &= \frac{mv_\perp^2}{2B(z)} = const. \end{aligned} \tag{5}$$

The condition for the axial confinement inside the magnetic mirror field is given by the following equation.

$$\frac{mv_{\perp 1}^2}{2} = \varepsilon - \mu B_1 - e\phi_1$$
$$= m\frac{v_0^2}{2} - \frac{B_1}{B_0}\frac{mv_{\perp 0}^2}{2} + e(\phi_0 - \phi_1) \quad (6)$$
$$= \frac{mv_{//0}^2}{2} - (R-1)\frac{mv_{\perp 0}^2}{2} + e\phi_c < 0$$

Therefore, the loss cone boundary is modified with the presence of the confinement potential $\phi_c = \phi_0 - \phi_1$ as follows.

$$sin^2\theta = \frac{1}{R}(1 + \frac{2e\,\phi_c}{mv_0^2}) \quad (7)$$

The schematics of the boundaries for protons and electrons are shown in FIG.4 for $\phi_c > 0$. In a simple magnetic mirror field, the ion confinement time $\tau_i \sim 1/\nu_{ii}$ and the electron confinement time $\tau_e \sim 1/\nu_{ee}$ are denoted by the ion-ion collision frequency ν_{ii} and electron-electron collision frequency ν_{ee}. Since ν_{ii} is much less than ν_{ee} in general, the electrons are scattered into the loss cone more rapidly than ions. Thus, the plasma becomes ion rich and ϕ_c becomes positive. This positive ϕ_c tends to confine electrons and expel ions as shown in FIG.4. As a result, the loss rates of ions and electrons balance at a certain point. This feature is called ambipolar diffusion. A mirror confined plasma observed in a large scale thermal fusion device [16] has a positive confinement potential $\phi_c \sim 100$ V with the plasma parameters listed in TABLE 2.

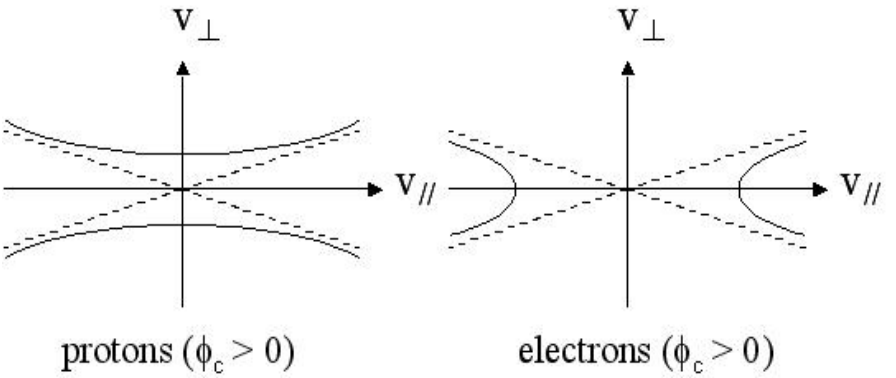

FIGURE 4. The schematics of loss cone distributions modified with the self filed potential $\phi_c > 0$, which are usually observed in a mirror confined plasma for thermonuclear fusion.

The confinement time in this case is expressed by [17]

$$\tau_M = 0.78\ \tau_i \ln\left[\frac{R}{1 + e\,\phi_c/T_i}\right] \quad with \quad \tau_i = \left(\frac{\pi}{2}\right)^{3/2} \frac{m^{1/2}k_B T_i^{3/2}}{ne^4 \ln\Lambda} \quad (8)$$

and is in the order of 10 msec. It should be noted in this example that the plasma is almost neutral. Excess protons are less than 10^{-4} of the plasma density. If the densities of both electrons and protons are reduced by four orders of magnitude, the confinement time seems to be much longer (~100 sec). However, the self field

potential ϕ_c is expected to be much smaller (~10 mV). Furthermore, protons and electrons are provided continuously by feeding hydrogen gas into the plasma. Obviously, these conditions are not fulfilled for low energy antiprotons and positrons. Some modifications are necessary for the simultaneous confinement of antiprotons and positrons.

TABLE 2. A hydrogen plasma in a magnetic mirror field

Plasma parameters	
Plasma density	n ~2 x 10^{12} cm^{-3}
Parallel Proton temperature	$T_{p//}$ ~ 400 eV
Perpendicular Proton temperature	$T_{p\perp}$ ~ 4 keV
Electron temperature	T_e ~ 80 eV

Simultaneous Confinement of Antiprotons and Positrons in a Magnetic Mirror Field

Here, the simultaneous confinement of antiprotons and positrons are considered in a simple magnetic mirror field. Compared with the previous example, the number of antiprotons and positrons are limited and their densities will be inevitably much smaller. Since the number of antiprotons is much more limited in experiments, it is assumed that there are much more positrons (10^8) than antiprotons (10^7) and that the density of positron is in the order of 10^6 to 10^8 cm^{-3}.

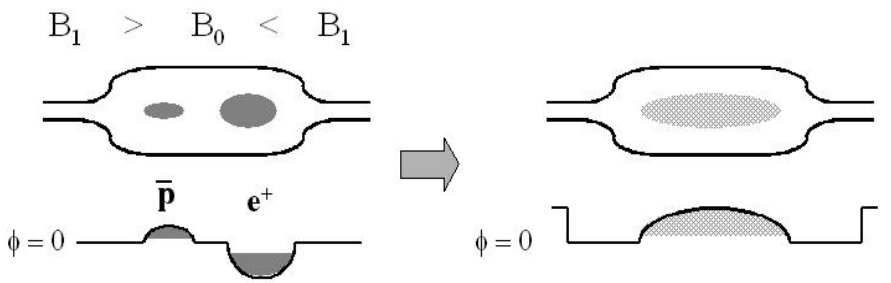

FIGURE 5. Antiprotons and positrons confined with a nested Penning trap inside a magnetic mirror field is mixed by the adiabatic expansion of both particles in axial direction.

The basic procedure for the simultaneous confinement is as follows. At first the low energy antiprotons and positrons are confined by a nested Penning trap inside a magnetic mirror field (FIG.5). Then, both particles are expanded adiabatically along the magnetic field by reducing the confinement potential. The adiabatic expansion results in anisotropic velocity distribution [18]. The perpendicular energy becomes larger than parallel energy, which enhances the particle confinement in the magnetic mirror field at the beginning. Since the excess positrons provide the confinement potential for antiprotons, both particles will be trapped simultaneously inside the

magnetic mirror field. The confinement potential ϕ_c of 1V will be necessary for 10^7 antiprotons.

The loss cone distribution will be modified as schematically shown in FIG.6 because there are much more positrons. In this case, the confinement time of low energy antiprotons is determined by the confinement time of positrons. This is because antiprotons are confined by the potential ϕ_c produced by positrons. As in the previous example, the confinement time of positrons in the magnetic mirror field is denoted by the collision frequency between positrons. When low energy positrons are confined in a strong magnetic mirror field, the collision frequency can be estimated [19]. A mirror ratio of 5 with B_0=1T and B_1=5T is a plausible example. Shown in FIG.7 is the calculated collision frequency for three different positron densities ranging from 10^6 to 10^8 cm^{-3}. It is seen that the lower density has the lower collision frequency, which leads to the longer confinement time. With the positron density of 10^6 cm^{-3} and the temperature of 1eV, the confinement time in a simple magnetic mirror field is expected to be less than 0.1 second. The strong magnetic field enhances the cyclotron radiation, which eventually moves positrons into the loss cone. Since the theoretical cyclotron radiation cooling time is about a few second for B_0=1T, its effect is not so serious in this case. It is thought that most of the characteristics of the antiproton-positron plasma can be investigated with the confinement time of 0.1sec.

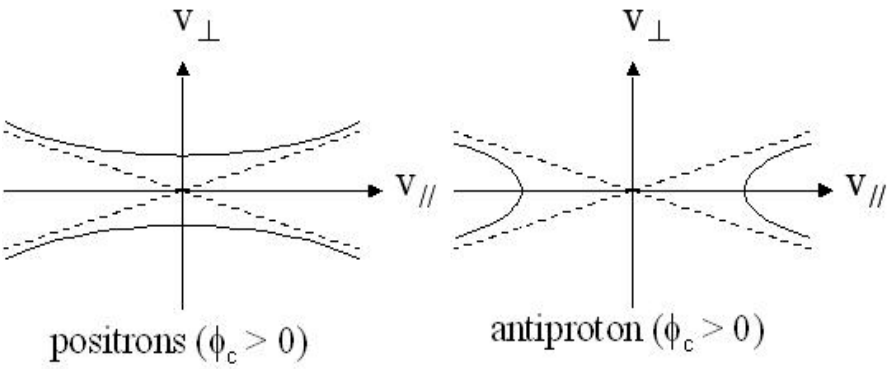

FIGURE 6. The schematics of loss cone distributions modified with the self filed potential ϕ_c >0, when much more positrons are confined than antiprotons.

If necessary, another technique should be employed to achieve a longer confinement time of the antiproton-positron plasma. One possibility is to apply positive electrostatic field outside the magnetic mirror as shown in FIG.4. This potential reflects back escaping positrons and the confinement time of the positrons can be much longer than the cyclotron radiation cooling time. However, this is not enough for the longer confinement of both particles. Since the confinement potential ϕ_c becomes the order of positron temperature [20], the low energy positrons (<0.1 eV) after the long confinement time results in the small ϕ_c for antiprotons. Therefore, the cyclotron resonance heating for positrons inside the magnetic mirror field by a small

power microwave will be necessary to keep the positron temperature of 1eV and confinement potential ϕ_c of 1V.

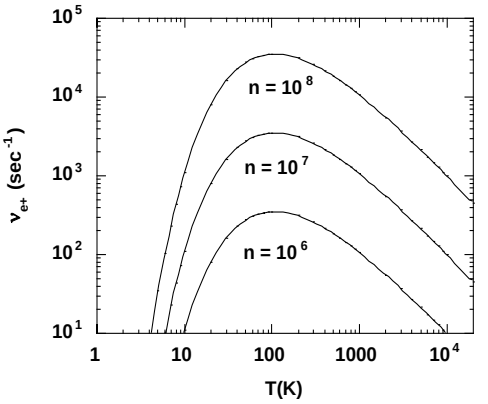

FIGURE 7. Calculated collision frequencies between positrons in a strong magnetic field (B=1T) for three different densities.

The same procedure is expected to work more effectively for the production of electron-positron plasma. In this case, equal densities of electrons and positrons can be confined simultaneously with the cyclotron resonance heating for both particles. Injection of moderated low energy positrons into the magnetic mirror field with the application of cyclotron resonance heating at the minimum B field may enhance the accumulation rate of low energy positrons in the trap without a buffer gas which was necessary to obtain 10^8 low energy positrons in a trap so far.

SUMMARY

Non-neutral antiproton plasmas will be realized near future. Proper manipulation of antiproton plasmas will be important for the effective production of low energy antiproton beams. Nondestructive measurement of the antiproton plasma with its electrostatic oscillations should be used as a real time monitor inside a trap. A magnetic mirror confinement may be used for the production of antiproton-positron plasmas and electron-positron plasmas.

ACKNOWLEDGMENTS

The author acknowledges the ASACUSA trap group members and those involved in AD, RFQD operation.

REFERENCES

1. G. Gabrielse, X. Fei, L. A. Orozco, S. L. Rolston, R. L. Tjoelker, T. A. Trainor, J. Haas, H. Kalinowsky, and W. Kells, *Phys. Rev. Lett.* **63**, 1360 (1989)
2. M. Amoretti *et al.*, *Nature* (London) **419**, 456 (2002).
3. N. Kuroda, H. A. Torii, K. Yoshiki Franzen, Z. Wang, S. Yoneda, M. Inoue, M. Hori, B. Juhasz, D. Horvath, H. Higaki, A. Mohri, J. Eades, K. Komaki, and Y. Yamazaki, *Phys. Rev. Lett.* **94** 023401 (2005).
4. G. Gabrielse *et al.*, *Phys. Rev. Lett.* **89**, 213401 (2002).
5. C. S. Weimer, J. J. Bollinger, F. L. Moore, and D. J. Wineland, *Phys. Rev. A* **49**, 3842 (1994).
6. H. Higaki, N. Kuroda, T. Ichioka, K. Yoshiki Franzen, Z. Wang, K. Komaki, Y. Yamazaki, M. Hori, N. Oshima, and A. Mohri, *Phys. Rev. E* **65** 046410 (2002)
7. T. B. Michell, J. J. Bollinger, X. -P. Huang, and W. M. Itano, *Opt. Express* **2** (1998) 314.
8. G. Dimonte, *Phys. Rev. Lett.* **46**, 26 (1981)
9. X. –P. Huang, F. Anderegg, E. M. Hollmann, C. F. Driscoll, And T. M. O'Neil, *Phys. Rev. Lett.* **78**, 875 (1997).
10. R. G. Greaves and C. M. Surko, *Phys. Rev. Lett.* **75** 3846 (1995).
11. K. Iwata, R. G. Greaves, T. J. Murphy, M. D. Tinkle, and C. M. Surko, *Phys. Rev. A* **51** 473 (1995).
12. N. Oshima, T. M. Kojima, M. Niigaki, A. Mohri, K. Komaki, and Y. Yamazki, *Phys. Rev. Lett.* **93**, 195001 (2004).
13. H. Higaki, N. Kuroda, K. Yoshiki Franzen, Z. Wang, M. Hori, A. Mohri, K. Komaki, and Y. Yamazaki, *Phys. Rev. E* **70** 026501 (2004)
14. K. Yoshiki Franzen, N. Kuroda, H. A. Torii, M. Hori, Z. Wang, H. Higaki, S. Yoneda, B. Juhasz, D. Horvath, A. Mohri, K. Komaki, and Y. Yamazaki, *Rev. Sci. Instrum.* **74** 3305 (2003).
15. F. F. Chen, Introduction to *Plasma Physics and Controlled Fusion*, New York: Plenum, 1984.
16. H. Higaki, M. Ichimura, K. Horinouchi, K. Nakagome, S. Kakimoto, Y. Yamaguchi, K. Ide, D. Inoue, H. Nagai, M. Yoshikawa, Y. Nakashima, and T. Cho, *Rev. Sci. Instrum.* **75** 4085 (2004).
17. D. V. Sivukhim, "Coulomb collisions in a fully ionized plasma," in *Reviews of Plasma Physics*, **4** edited by M. A. Leontovich, New York: Consultants Bureau, 1966, pp. 93-241.
18. A. W. Hyatt, C. F. Driscoll, and J. H. Malmberg, *Phys. Rev. Lett.* **59** (1987) 2975
19. B. R. Beck, J. Fajans, and J. H. Malmberg, *Phys. Rev. Lett.* **68** (1992) 317.
20. J. Fajans, *Phys. Plasmas* **10** 1209 (2003).